J. Cent. South Univ. (2018) 25: 831−842
DOI: https://doi.org/10.1007/s11771-018-3787-7

Springer

Theoretical and experimental investigation on internal gear pair with small sliding ratio

PENG Shuai(彭帅)[1], MA Zhi-fei(马志飞)[2, 3], CHEN Bing-kui(陈兵奎)[1],
QIN Si-ling(覃思玲)[1], WANG Shu-yan(王淑妍)[4]

1. State Key Laboratory of Mechanical Transmission, Chongqing University, Chongqing 400030, China;
2. Aerospace System Engineering Shanghai, Shanghai Academy of Spaceflight Technology, Shanghai 201100, China;
3. Shanghai Key Laboratory of Spacecraft Mechanism, Shanghai Academy of Spaceflight Technology, Shanghai 201100, China;
4. School of Mechanical Engineering, Jiangsu University of Science and Technology, Zhenjiang 212003, China

Abstract: Aiming at the issue of sliding ratio, an internal gear pair is proposed which consists of an involute internal gear and a pinion with quadratic curve teeth. Particularly, the contact pattern is point contact and the pinion is generated based on an involute gear. The generation method and mathematical models of the gear pair are presented. The sliding ratio is calculated and the general calculation formulas of sliding ratios are developed. Also, the comparison between the involute gear and proposed gear is made. The adaptability of center distance and contact stress are also discussed. In addition, the gear pair was manufactured and inspected according to the exactitude solid model of the gear pair. In order to confirm this model to be effective, the efficiency experiment and the contrast experiment with the involute gear pair were performed. Furthermore, these two types of pinions were analyzed by scanning electron microscope and wear depths were measured by measuring center. The experiment results show that the efficiency of the internal gear pair is stable at a range about 97.1% to 98.6% and wear depth is less than 50% of the involute gear pair. The internal gear pair is expected to have excellent transmission performance.

Key words: internal gear; sliding ratio; quadratic curve; wear

Cite this article as: PENG Shuai, MA Zhi-fei, CHEN Bing-kui, QIN Si-ling, WANG Shu-yan. Theoretical and experimental investigation on internal gear pair with small sliding ratio [J]. Journal of Central South University, 2018, 25(4): 831–842. DOI: https://doi.org/10.1007/s11771-018-3787-7.

1 Introduction

Internal gear pair has been widely applied in gear boxes such as planetary mechanisms, aerospace and differential mechanisms due to the advantages of low contact stress and high contact ratios compared with external gear pair [1]. Tooth profile plays an important part in transmission performance. It is not only the direct factor that influences the transmission efficiency, load capacity and relative motion characteristics, but also the main factor that influences the vibration, noise and reliability. To search for new tooth profiles, many researchers have done much work [2–5].

As for contact pattern of internal gears, line

Foundation item: Project(51575062) supported by the National Natural Science Foundation of China; Project(SM2014D202) supported by the Fund of Shanghai Key Laboratory of Spacecraft Mechanism, China
Received date: 2016−11−21; **Accepted date:** 2017−01−23
Corresponding author: CHEN Bing-kui, PhD, Professor; Tel: +86–23–65106247; E-mail: bkchen@cqu.edu.cn; ORCID: 0000-0002-5790-0670

contact pattern is the most commonly used. Involute gears are applied all over the world because of the convenience of manufacturing and low assembly accuracy [6]. Gears with point contact pattern have been developed over the decades. They have the advantages of high contact strength, high efficiency and low noise. In particular, as for internal gears, ZHANG et al [7] provided a new method of calculating the profile of the gear tooth of the straight conjugate internal meshing gear pump. XU [8] proposed a double-circular-arc gear with inner meshing. KAHRAMAN et al [9] investigated the effect of flexibility of an internal gear on the quasi-static behavior of a planetary gear set. TUNALIOGLU et al [10] investigated the wear in internal gears at different conditions by using Archard's wear modified equation and a MATLAB program.

During the transmission process, the meshing surfaces of gears slide relatively because of the different velocities at contact area. Sliding ratio is one of the key factors that determine the degree of wear under low speed, and is a main noise source. By now, some researches concerning the problem have been carried out. LI et al [11] studied the sliding ratios of the tooth surfaces of the spherical gear pairs with two degrees of freedom. WANG et al [12] proposed a method of the preliminary geometric design for gear tooth profiles based on given sliding coefficients. CHEN [13] studied the sliding velocities and sliding ratios of the conjugate surfaces. LIANG et al [14] proposed the calculation method of sliding ratios for conjugate-curve gear pair. ZHAO et al [15] calculated the sliding ratio of crossed helical involute gear pair by using the formula deduced for spot contact tooth surfaces. WANG [16] analyzed the sliding velocity between the standard spur gear teeth. ZHANG [17] developed the relative sliding ratio formulas of involute spur gear pair.

In this work, an internal gear pair with small sliding ratio is proposed which consists of an involute internal gear and a pinion with quadratic curve teeth. Particularly, the contact pattern is point contact and the proposed pinion is generated based on an involute one. Thus, the gear pair inherits the characteristic of adaptability of center distance error, which is the prominent feature of involute gear. To interpret the mesh principle of the proposed internal gear pair, the generation method of the gear pair is presented. The mathematical models of the tooth surfaces are deduced. The adaptability of center distance and contact stress are discussed. The sliding ratio is calculated and the comparison between the involute gear and proposed gear is made. According to the exactitude solid model, the gear pair was manufactured and inspected. The efficiency experiment and the contrast experiment with the involute gear pair were performed. The discussions are provided. It is expected that more insights into processing method and performance could be gained through this study and parametrical design and utilization of this gar pair could be achieved.

2 Mathematical model of internal gear pair

The tooth surface of the pinion proposed in this work is generated by using the following methods: 1) Suppose an involute pinion is given and the tooth surface Σ_1 is determined; 2) Selecting a smooth curve on the given tooth surface near the pitch line and the equation of the curve Γ_1 can be derived; 3) New tooth surface is generated based on a family of continuously variable plane curves along curve Γ_1. The plane curve, i.e., the tooth profile, is a quadratic curve and tangent to the given surface Σ_1. 4) The internal gear is designed with an involute gear which has the same module and helical angle.

2.1 Equation of contact path on pinion

As shown in Figure 1, $S_0(O_0–x_0, y_0, z_0)$ and $S_p(O_p–x_p, y_p, z_p)$ are the fixed coordinate systems rigidly connected to the absolute space. Movable coordinate systems $S_1(O_1–x_1, y_1, z_1)$ and $S_2(O_2–x_2, y_2, z_2)$ are rigidly connected to the pinion and the gear, respectively. The two gears rotate in the same direction around axis z_0 with an instantaneous angular velocity ω_1 and ω_2. O_0 O_p is the center distance a and P_t is the contact point.

The equation of tooth surface of involute pinion Σ_1 in coordinate system S_1 can be expressed as:

$$\Sigma_1=\begin{cases}x_1=r\cos(\theta+\alpha)+r\theta\sin(\theta+\alpha)\\ y_1=r\sin(\theta+\alpha)-r\theta\cos(\theta+\alpha)\\ z_1=p\alpha\end{cases} \tag{1}$$

A tooth surface can be generated by a screw

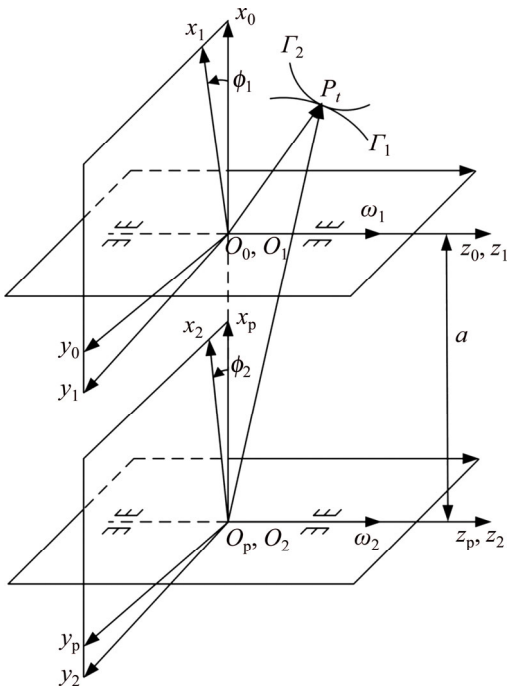

Figure 1 Coordinate systems of internal gear pair

motion of the profile about the gear axis [18]. For most gears, the screw motion is usually a circular helix, such as involute gear and circular arc gear. In this work, the trail of screw motion, i.e., the contact path, is a curve selected on the tooth surface of the involute pinion and is a combination of involute and helix as shown in Figure 2. The curve can be any shape which depends on the relationship between θ and α. To make it simple, we assumed that there is a linear relationship between θ and α. The expression can be written as:

$$\Gamma_1=\begin{cases}x_{\Gamma 1}=r\cos(\theta+\alpha)+r\theta\sin(\theta+\alpha)\\ y_{\Gamma 1}=r\sin(\theta+\alpha)-r\theta\cos(\theta+\alpha)\\ z_{\Gamma 1}=p\alpha\\ \alpha=k\theta+b\end{cases} \tag{2}$$

where $k=\dfrac{B}{p(\theta_2-\theta_1)}$, $b=-\dfrac{\theta_1 B}{p(\theta_2-\theta_1)}$, the range of involute parameter θ is $\theta_2\leq\theta\leq\theta_1$, θ_1 and θ_2 are the boundary conditions, i.e., initial value and final value of θ.

2.2 Equation of pinion tooth surface

A tooth profile determines the kinetic and dynamical properties of a gear pair. In this work, a new profile, quadratic curve, is used as the tooth profile.

Figure 3 illustrates the generation process of the pinion tooth surface. Assuming that $\boldsymbol{\beta}_1$, $\boldsymbol{\alpha}_1$ and $\boldsymbol{\gamma}_1$ construct a coordinate system denoted by S_c and represent x-axis, y-axis and z-axis, respectively, where $\boldsymbol{\beta}_1$, $\boldsymbol{\alpha}_1$ and $\boldsymbol{\gamma}_1$ demonstrate the principal normal vector, tangent vector and binormal vector of curve Γ_1 in coordinate system S_1 and $\boldsymbol{\beta}_1$ is also the normal vector of Σ_1. Contact point P_t is set to be the coordinate origin.

According to the knowledge of geometry, $\boldsymbol{\beta}_1$, $\boldsymbol{\alpha}_1$ and $\boldsymbol{\gamma}_1$ can be written as:

$$\begin{cases}n_{x\beta}=-pr\theta\sin[(k+1)\theta+b]\\ n_{y\beta}=pr\theta\cos[(k+1)\theta+b]\\ n_{z\beta}=-r^2\theta\end{cases} \tag{3}$$

$$\begin{cases}n_{x\alpha}=r\{(1+k)\theta\cos[(k+1)\theta+b]+\sin[(k+1)\theta+b]-\\ \qquad(1+k)\sin[(k+1)\theta+b]\}\\ n_{y\alpha}=r\{-\cos[(k+1)\theta+b]+(1+k)\cos[(k+1)\theta+b]+\\ \qquad(1+k)\theta\sin[(k+1)\theta+b]\}\\ n_{z\alpha}=kp\end{cases} \tag{4}$$

$$\begin{cases}n_{x\gamma}=n_{y\beta}n_{z\alpha}-n_{y\alpha}n_{z\beta}\\ n_{y\gamma}=n_{z\beta}n_{x\alpha}-n_{z\alpha}n_{x\beta}\\ n_{z\gamma}=n_{x\beta}n_{y\alpha}-n_{x\alpha}n_{y\beta}\end{cases} \tag{5}$$

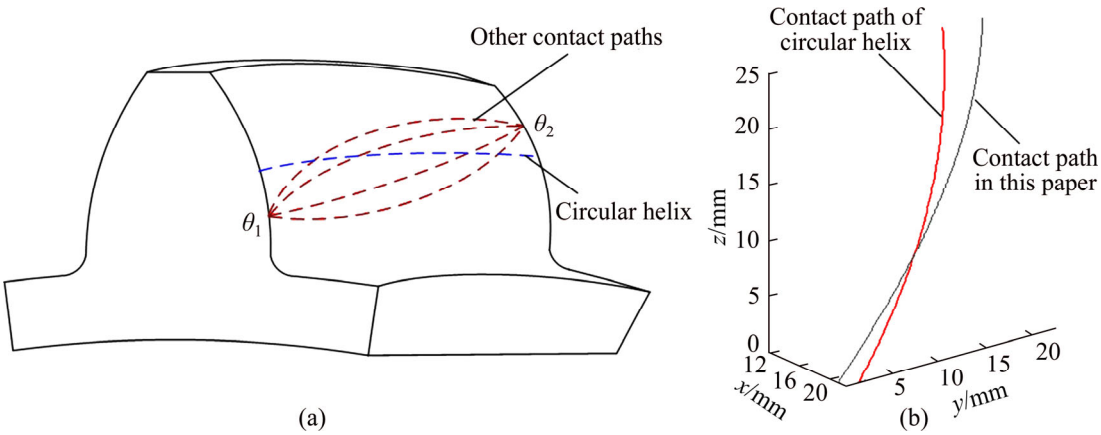

Figure 2 Selecting of contact path (a) and comparison of contact paths (b)

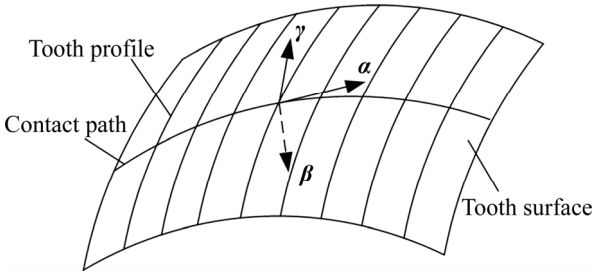

Figure 3 Generation of tooth surface

The unit vectors can be written as:

$$\begin{cases} n_{nx\beta}=\dfrac{n_{x\beta}}{\sqrt{n_{x\beta}^2+n_{y\beta}^2+n_{z\beta}^2}} \\ n_{ny\beta}=\dfrac{n_{y\beta}}{\sqrt{n_{x\beta}^2+n_{y\beta}^2+n_{z\beta}^2}} \\ n_{nz\beta}=\dfrac{n_{z\beta}}{\sqrt{n_{x\beta}^2+n_{y\beta}^2+n_{z\beta}^2}} \end{cases} \tag{6}$$

$$\begin{cases} n_{nx\alpha}=\dfrac{n_{x\alpha}}{\sqrt{n_{x\alpha}^2+n_{y\alpha}^2+n_{z\alpha}^2}} \\ n_{ny\alpha}=\dfrac{n_{y\alpha}}{\sqrt{n_{x\alpha}^2+n_{y\alpha}^2+n_{z\alpha}^2}} \\ n_{nz\alpha}=\dfrac{n_{z\alpha}}{\sqrt{n_{x\alpha}^2+n_{y\alpha}^2+n_{z\alpha}^2}} \end{cases} \tag{7}$$

$$\begin{cases} n_{nx\gamma}=\dfrac{n_{x\gamma}}{\sqrt{n_{x\gamma}^2+n_{y\gamma}^2+n_{z\gamma}^2}} \\ n_{ny\gamma}=\dfrac{n_{y\gamma}}{\sqrt{n_{x\gamma}^2+n_{y\gamma}^2+n_{z\gamma}^2}} \\ n_{nz\gamma}=\dfrac{n_{z\gamma}}{\sqrt{n_{x\gamma}^2+n_{y\gamma}^2+n_{z\gamma}^2}} \end{cases} \tag{8}$$

Then, the tooth profile in coordinate system S_c can be expressed as

$$\Gamma(t)=(x_c,y_c,z_c,1)^{\mathrm{Tr}}=(k_1t^2 \quad 0 \quad k_1t \quad 1)^{\mathrm{Tr}} \tag{9}$$

From the expression, it is obvious that the tooth profile is a quadratic curve.

After three coordinate axes are derived, the equation of the pinion in S_1 is deduced as:

$$\begin{cases} x_{\Sigma_1}=n_{x\beta}x_c+n_{x\alpha}y_c+n_{x\gamma}z_c+x_{\Gamma_1} \\ y_{\Sigma_1}=n_{y\beta}x_c+n_{y\alpha}y_c+n_{y\gamma}z_c+y_{\Gamma_1} \\ z_{\Sigma_1}=n_{z\beta}x_c+n_{z\alpha}y_c+n_{z\gamma}z_c+z_{\Gamma_1} \end{cases} \tag{10}$$

2.3 Meshing equation

The relative velocity of the two gears in coordinate system S_2 is expressed as follows:

$$\begin{aligned} \boldsymbol{v}_2^{(12)}=&[-(\omega_1-\omega_2)y_2-a\omega_1\sin\phi_2]\boldsymbol{i}_2+ \\ &[(\omega_1-\omega_2)x_2-a\omega_1\cos\phi_2]\boldsymbol{j}_2 \end{aligned} \tag{11}$$

Then, the meshing equation is achieved:

$$\boldsymbol{v}_2^{(12)}\cdot\boldsymbol{n}_2=0 \tag{12}$$

where $\boldsymbol{n}_2$ is the normal vector of given surface Σ_1 at contact point and has been derived in Eq. (3).

Substituting Eq. (3) and Eq. (11) into Eq. (12), the meshing equation is expressed as:

$$A\sin(\phi_1)+B\cos(\phi_1)=M \tag{13}$$

where $A=i_{12}an_{x2}$, $B=i_{12}an_{y2}$, $M=(i_{12}-1)(x_2n_{y2}-y_2n_{x2})$, $\phi_1=i_{12}\phi_2$.

2.4 Equation of contact path on internal gear and line of action

According to kinematics and meshing theory [19], the contact path on tooth surface of the internal gear can be deemed as the envelope of curve Γ_1 in coordinate system S_1 and the contact points on two curves satisfy the meshing equation. The equation of conjugated curve Γ_2 on internal gear is expressed as

$$\Gamma_2=\begin{cases} x_{\Gamma_2}=\cos(\phi_1-\phi_2)x_{\Gamma_1}-\sin(\phi_1-\phi_2)y_{\Gamma_2}+a\cos(\phi_2) \\ y_{\Gamma_2}=\sin(\phi_1-\phi_2)x_{\Gamma_1}+\cos(\phi_1-\phi_2)y_{\Gamma_2}-a\sin(\phi_2) \\ z_{\Gamma_2}=z_{\Gamma_1} \\ A\sin\phi_1+B\cos\phi_1=M \end{cases} \tag{14}$$

Line of action is defined as the set of the instantaneous contact points between two mating tooth profiles in the fixed coordinate system. Utilizing coordinate transformation from movable coordinate system S_1 to fixed coordinate system S_0, the equation of line of action can be obtained as:

$$\begin{cases} x=x_1\cos\phi_1-y_1\sin\phi_1 \\ y=x_1\sin\phi_1+y_1\cos\phi_1 \\ z=z_1 \end{cases} \tag{15}$$

3 Sliding ratio of gear pair

Sliding ratio is one of the key factors which determine the degree of the gear tooth wear. It is the ratio of the relative sliding velocity to the velocity of the contact point on each tooth profile when the

gears are in mesh and the relative sliding velocities are different at the contact point.

According to Refs. [17] and [20], the sliding ratio of an involute gear is zero at the pitch line, close to zero near the pitch line, and gradually increase to the tooth tip and tooth root direction as shown in Figure 4. As mentioned in Section 1, the proposed pinion is generated based on an involute one. In this work, the contact path is selected on the given tooth surface and the range of the contact path is near the area of pitch line. Therefore, the sliding ratio of the proposed gear pair mainly depends on the range of the contact path and it can be very small in the condition of the range is near and across the pitch line.

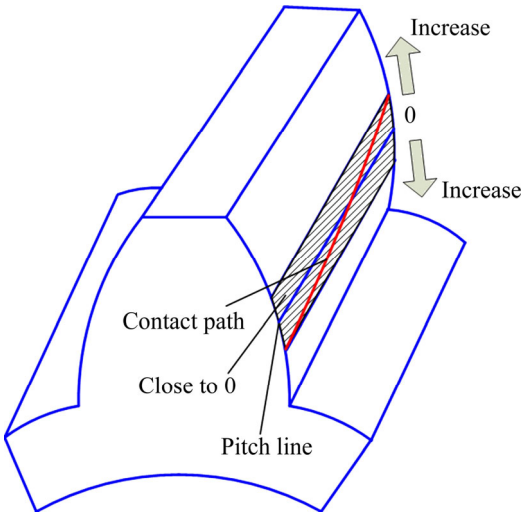

Figure 4 Sliding ratio of involtue gear

Based on the calculation method [14], the sliding ratio of gears η, of which contact pattern is point contact, can be obtained as a ratio of the length which the contact point of a gear moves at a short time that approaches to zero to that of the mating gear. Therefore, it can be expressed as

$$\eta_1 = \lim_{\Delta S_1 \to 0} \frac{\Delta S_1 - \Delta S_2}{\Delta S_1} = \frac{\dfrac{\mathrm{d}S_1}{\mathrm{d}\theta} - \dfrac{\mathrm{d}S_2}{\mathrm{d}\theta}}{\dfrac{\mathrm{d}S_1}{\mathrm{d}\theta}} = \lim_{\Delta S_1 \to 0} \frac{\mathrm{d}S_1 - \mathrm{d}S_2}{\mathrm{d}S_1} \tag{16}$$

$$\eta_2 = \lim_{\Delta S_2 \to 0} \frac{\Delta S_2 - \Delta S_1}{\Delta S_2} = \frac{\dfrac{\mathrm{d}S_2}{\mathrm{d}\theta} - \dfrac{\mathrm{d}S_1}{\mathrm{d}\theta}}{\dfrac{\mathrm{d}S_2}{\mathrm{d}\theta}} = \lim_{\Delta S_2 \to 0} \frac{\mathrm{d}S_2 - \mathrm{d}S_1}{\mathrm{d}S_2} \tag{17}$$

where

$$\mathrm{d}S_1 = \sqrt{\mathrm{d}x_{\Gamma_1}^2 + \mathrm{d}y_{\Gamma_1}^2 + \mathrm{d}z_{\Gamma_1}^2}\,\mathrm{d}\theta \tag{18}$$

$$\mathrm{d}S_2 = \sqrt{\mathrm{d}x_{\Gamma_2}^2 + \mathrm{d}y_{\Gamma_2}^2 + \mathrm{d}z_{\Gamma_2}^2}\,\mathrm{d}\theta \tag{19}$$

Substituting Eqs. (2) and (14) into Eqs. (18) and (19), it can be obtained that:

$$\begin{cases} \dfrac{\mathrm{d}x_1}{\mathrm{d}\theta} = r[(1+k)\theta\cos(\alpha+\theta) - k\sin(\alpha+\theta)] \\ \dfrac{\mathrm{d}y_1}{\mathrm{d}\theta} = r[k\cos(\alpha+\theta) + (1+k)\sin(\alpha+\theta)] \\ \dfrac{\mathrm{d}z_1}{\mathrm{d}\theta} = kp \end{cases} \tag{20}$$

$$\begin{cases} \dfrac{\mathrm{d}x_2}{\mathrm{d}\theta} = c_{2t}x_1 + c_2x_1' - c_{1t}y_1 - c_1y_1' - 1/i_{12}a\phi'(\theta)\sin(1/i_{12}\phi_1) \\ \dfrac{\mathrm{d}y_2}{\mathrm{d}\theta} = c_{1t}x_1 + c1x_1' + c_{2t}y_1 - c_2y_1' + 1/i_{12}a\phi'(\theta)\cos(1/i_{12}\phi_1) \\ \dfrac{\mathrm{d}z_2}{\mathrm{d}\theta} = kp \end{cases} \tag{21}$$

where

$$c_1 = \sin[(1-1/i_{12})\phi_1]$$

$$c_{1t} = (1-1/i_{12})\cos[(1-1/i_{12})\phi_1]\phi'(\theta)$$

$$c_2 = \cos[(1-1/i_{12})\phi_1]$$

$$c_{2t} = -(1-1/i_{12})\sin[(1-1/i_{12})\phi_1]\phi'(\theta)$$

$$\phi'(\theta) = \frac{1}{\sqrt{1-\dfrac{M^2}{A^2+B^2}}}\left(\frac{M}{\sqrt{A^2+B^2}}\right)' + \frac{1}{1+\left(\dfrac{A}{B}\right)^2}\left(\frac{A}{B}\right)'$$

Substituting Eqs. (20) and (21) into calculation formulas, the sliding ratio of proposed gear pair can be obtained. The computational procedure has been implemented in MATLAB in terms of design parameters in Table 1. The simulation results of the sliding ratios are shown in Figure 5(a). The sliding ratios of the involute gear which has the same design parameters are also calculated [17] and shown in Figure 5(b). According to the two pictures, it can be concluded that the range of sliding ratios

Table 1 Geometrical parameters of gear drive

Parameter	Value
Normal module, m_n/mm	4
Pressure angle on pitch circle, α/(°)	22.147
Teeth number of pinion, z_1	18
Teeth number of gear, z_2	267
Tooth width, B	25
Independent variable range of curve, θ/rad	[0.31,0.62]
Hand of helix	Right-hand

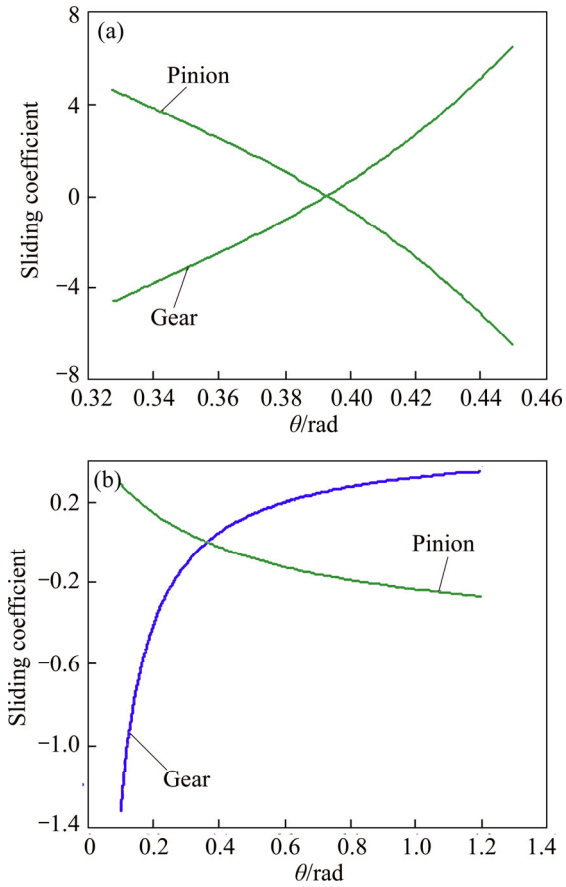

Figure 5 Sliding ratio of two kinds of gears: (a) Sliding ratio of proposed internal gear pair; (b) Sliding ratio of involute gear

of the new internal gear is $\pm 6\times10^{-3}$, which is very close to zero, in the theoretical condition, whereas that of involute gear pair is from –1.2 to 0.4. Compared with the two results, it is obvious that the sliding ratio of the proposed internal gear pair is much less than that of involute gear pair. Therefore, the application of the new internal gear drive can reduce the sliding ratio efficiently and improve the transmission performance.

4 Evaluation of internal gear pair

4.1 Solid model and motion simulation

The three-dimensional solid model can be established by using computer software. In this paper, the solid model is established by using MATLAB and solid modeling software UG. The solid models of the gear pair are established as shown in Figure 6.

As shown in Figure 7, the simplified internal gear and pinion tooth surfaces are given. Line of action is depicted as a straight line. The engagement

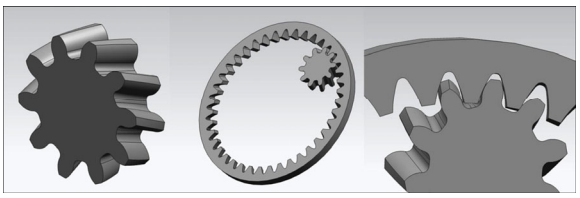

Figure 6 Solid model of internal gear pair

of tooth surfaces at the initial position is displayed in Figure 7(a). When the gear pair rotates with an angular velocity, the tooth surfaces come in contact with each other in the contact point P_t. The meshing condition at arbitrary position is described in Figure 7(b). During the transmission process, the internal gear and pinion tooth surfaces mesh are in point contact. The instantaneous contact point of tooth surfaces moves along the line of action.

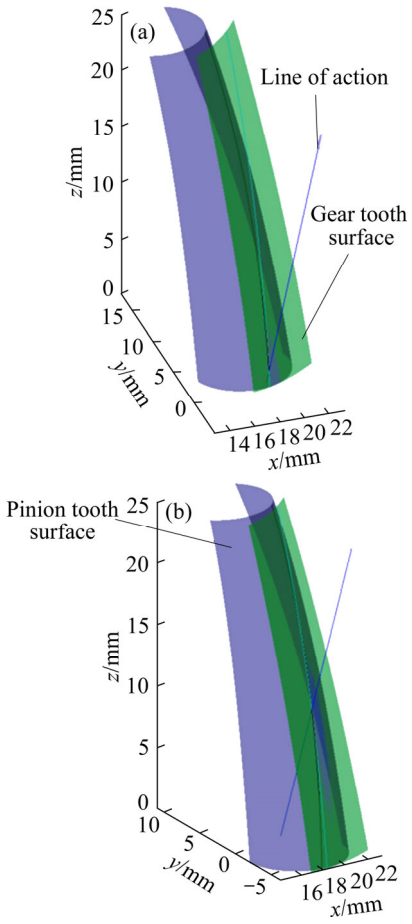

Figure 7 Meshing schematic of tooth surfaces: (a) Initial position; (b) Arbitrary position

In Figure 8, the motion simulation of the meshing process is conducted in UG. It is obvious that in the whole process of mesh, the contact pattern is point contact and the contact point moves along the theoretical contact path.

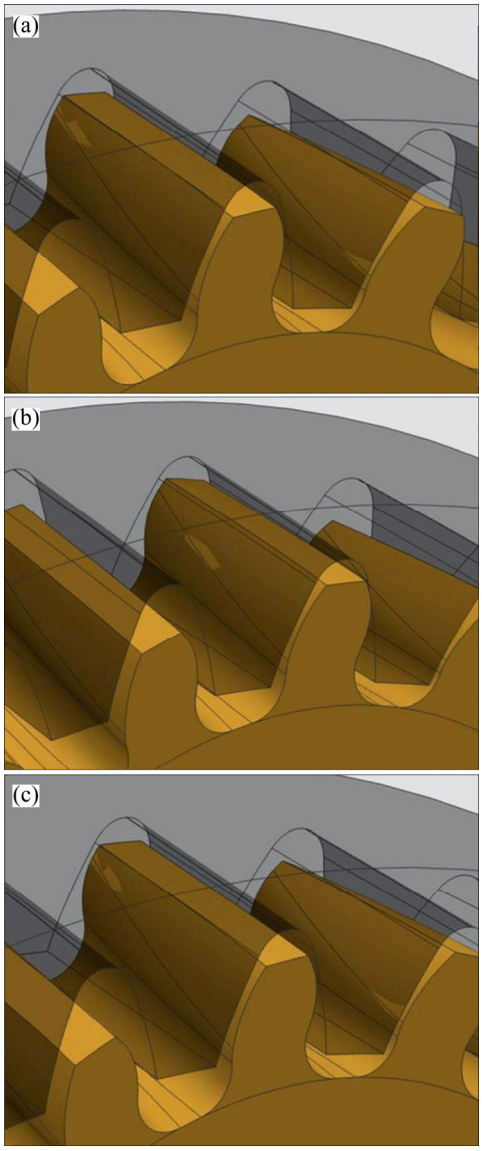

Figure 8 Motion simulation of internal gear pair: (a) ϕ=0°; (b) ϕ=10°; (c) ϕ=20°

4.2 Adaptability to center distance variation

It is one of the advantages of the involute gear that the instantaneous transmission ratio remains unchanged, while center distance of the gear pair changes slightly. The proposed internal gear transmission also can adapt the change of the center distance due to uniqueness of the contact path. As shown in Figure 9, according to the aforementioned description, the contact path on the pinion is also a curve which is on an involute surface. Assuming that the involute surface is used as the reference surface which is engaged with the gear surface, then, the mesh of the proposed gear pair can be regarded as that of two involute gears. Therefore, the contact path can inherit the characteristic of the involute surface and adapt the center distance variation.

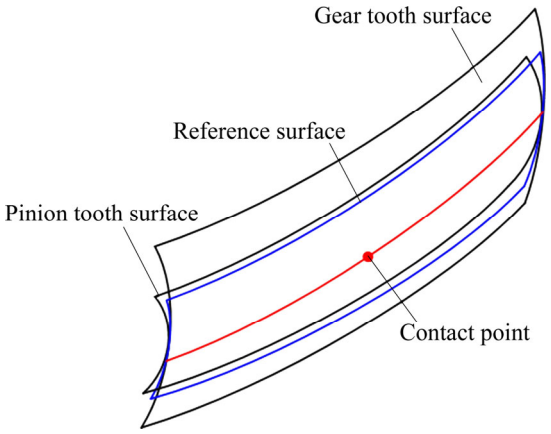

Figure 9 Illustration of mesh

4.3 Contact stress

This section presents the analysis of contact stress of the proposed internal gear pair by using the finite element analysis (FEA) software ANSYS [21]. Through this analysis, the mechanical characteristics of these gears can be evaluated.

The numerical computations have been performed with the design parameters in Table 1 and the solid models are established according to Section 2. From the solid model, a 3-pair-of-teeth finite element model is built shown in Figure 10(a). In this model, there are 120704 elements with 122587 nodes. The torque applied to the gear is 60 N·m. Besides, the material is set as steel and properties of materials are: μ=0.29, E=2.05×10^5 MPa.

From the results of finite element analysis, the variations of max contact stresses on the central pair of teeth in a meshing cycle have been studied. Figures 10(b) and (c) show the variations of max contact stresses the central pair of teeth. According to the results of finite element analysis, the maximum of contact stress in the meshing process is 406 MPa. Compared with the allowable stress of steel, which is about 800 MPa, it is much smaller than the allowable stress.

4.4 Manufacturing and inspection

According to the mathematical model, the gear pair was manufactured and used for experimental studies. With the development of numerical control technology, the manufacture of complicated surface can be realized [22, 23]. Considering the processing method and stability of the machine, the pinion was manufactured by using 5-axis machining center, DMU 60. It is of good working accuracy and

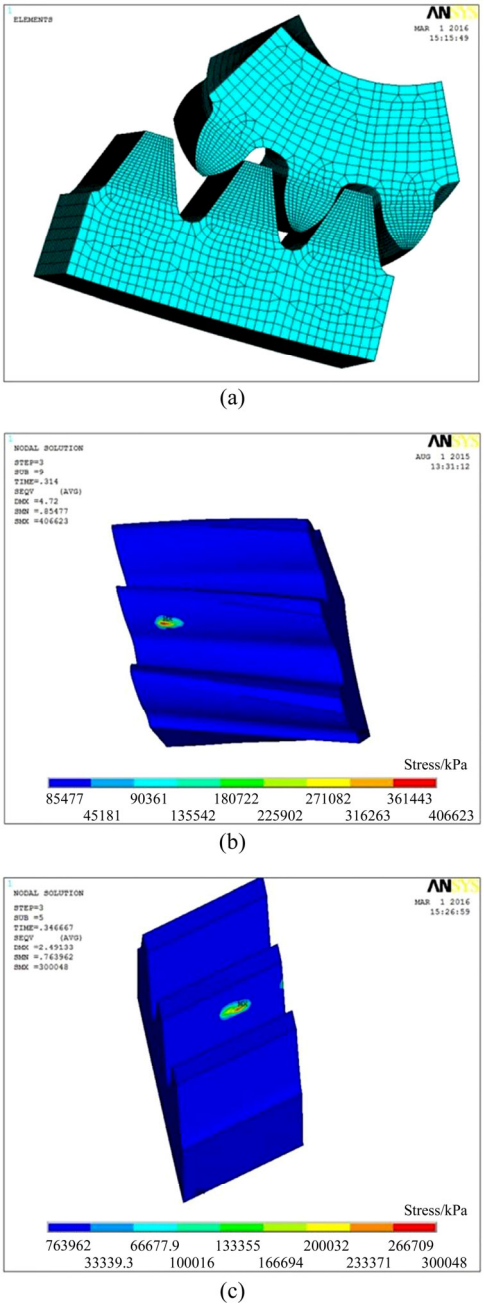

Figure 10 Finite element analysis: (a) Finite element model; (b) Contact stress of pinion; (c) Contact stress of internal gear

operability. The processing technique of the involute gear has been well developed over the years. For internal gears, gear shaping is the common method due to its high production rates. In this work, as the module is small, the internal gear was manufactured by grinding which is of high accuracy. The geometrical properties and the heat treatment of gear pair are given in Tables 1 and 2, respectively.

It is inevitable that deviation occurs between the processed gear and the theoretical model [24].

Table 2 Material and heat treatment of gear pair

Part	Material	Heat treatment	Hardness
Pinion	05Cr15Ni5Cu4Nb	Solution treatment	HRC41–45
Internal gear	42CrMo	Hardening and tempering	HRC 35–39

The internal gear was inspected by measuring the common normal length, profile tolerance and so on. As the pinion is a new type of gear, the inspection method is not well developed like the involute gear. To validate the deviation, the pinion was inspected on measuring center to obtain the coordinate values of different points on the tooth surface on different cross-sections, as shown in Figure 11. Then compare the value obtained by the measuring center with that obtained by MATLAB, thus, the deviation is derived. Table 3 shows the deviations of different cross-sections of the pinion.

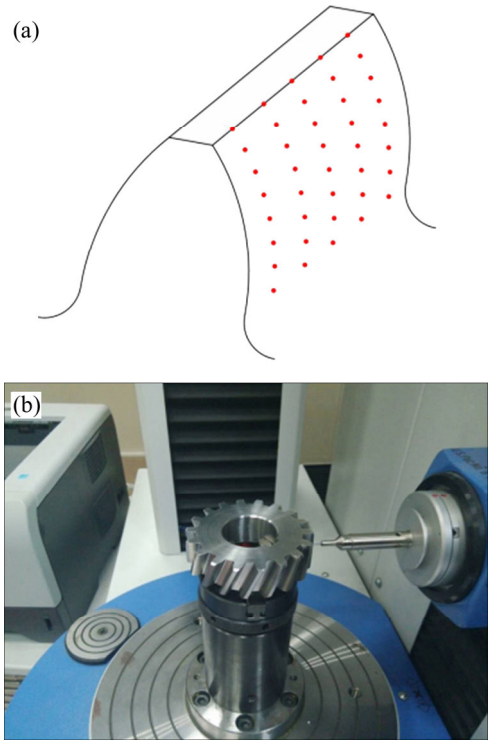

Figure 11 Measuring points from tooth profile (a) and measuring points on measuring center (b)

Table 3 Deviations of different cross-sections of pinion

Cross-section number	Average deviation/μm	Maximum deviation/μm
1	1.82	2.05
2	1.78	1.95
3	1.86	2.14
4	1.80	1.99
5	1.83	2.01

5 Performance experiment

5.1 Test rig

To investigate the transmission performance of the gear drive, a gear drive test rig was designed and could be used to investigate the transmission efficiency of this new gear drive.

A servo motor was used as the power source in the test rig. The input and output torques and rotational speeds were measured by torque and rotational speed transducer. The test rig was loaded by a magnetic powder brake. The servo motor, the input transducer and the pinion were united on a stand. Lubricant grease was used in the experiment. The components of test rigs were linked by couplings.

5.2 Test procedure

Due to the elastic deformations, the contact point will spread over a small area. Considering the point contact pattern of the internal gear pair, the running-in process was carried out to expand the contact area and modify the tooth surface for increasing the load capacity and reducing noise and vibration. The running-in process lasted for 8 h. The first 4 h ran with an input speed of 60 r/min, and the next 4 h ran with an input speed of 60 r/min and an output torque of 60 N·m. After 8 h running-in process, the gear pair was considered to be under an ideal contact situation.

To investigate the transmission efficiency, the test rig is operated in different motor speeds (30, 60, 90 and 120 r/min) and different output torsional moments (30 N·m to 100 N·m). The system was stopped after 8.8×10^4 revolutions of the internal gear. The contrast experiment of the involute gear pair with the same design parameters and processing method under the same working conditions was also performed.

5.3 Results and discussion

5.3.1 Efficiency

After the experiments, the contact path can be clearly seen in Figure 12, which validates the correctness of the mathematical model.

The transmission efficiency of the new gear and the involute gear is shown in Figure 13. It is possible to note that:

1) When the torque is constant, the efficiency increases with the rotational speed. Similarly, when the rotational speed is constant, the efficiency increases with the torque.

2) The efficiency of the new internal gear is stable at a range about 97.1% to 98.6%, which is about 0.35% higher than that of the involute gears. Besides, the precision of the test rig and the assembly errors may also affect the transmission efficiency. Further study on precision manufacturing will be worked out.

Figure 12 Contact path of pinion

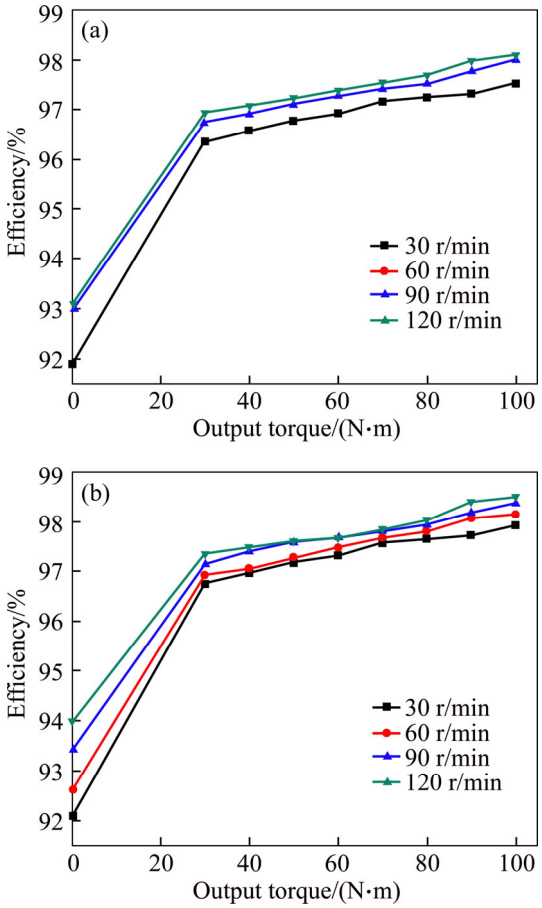

Figure 13 Transmission efficiency of involute gears (a) and proposed gears (b)

5.3.2 Variation of wear depth

As the revolutions of the pinion is much larger than that of the internal gear, wear depth of two pinions are measured by measuring center [10]. The comparison of wear depth graphics of involute pinion and proposed pinion is given in Figure 14. As for the involute pinion, wear occurs on the whole tooth surface, while that of the proposed pinion occurs only at the area of the contact path. Since the sliding ratio is zero on the pitch line, there is no wear at this point. Wear depth value increases with the increase of output torsional moment and motor speed. It is noted that wear increases along the tooth tip and tooth root and the maximum wear occurs on the tooth root where mesh begins with the pinion, which is agreeable with the theoretical calculation result in Figure 5.

Sliding ratio influences the degree of wear. Large sliding ratio means high relative sliding velocity and more wear depth of gear surfaces, which affects the life time of the gears. According to Figure 14, wear depth of the proposed pinion is less than 50% of the involute gear pair at any conditions of output torsional moment and motor speed, which is because small sliding ratio can reduce wear and approximately pure rolling is realized instead of sliding.

Besides, the two pinions were both analyzed by scanning electron microscope after the experiment to investigate the roughness of the tooth surfaces. One tooth is cut off from the two pinions respectively and scanned by scanning electron microscope to observe surface topography at a magnification of 300 times. The results are shown in Figure 15. Two conclusions can be drawn:

1) After the experiment, the contact region of the proposed gear becomes smoother than the uncontact region. However, mild wear occurs on the involute tooth surface after the experiment. This is because the point contact pattern makes the new gear pair have the advantage of low sliding ratio which can reduce wear.

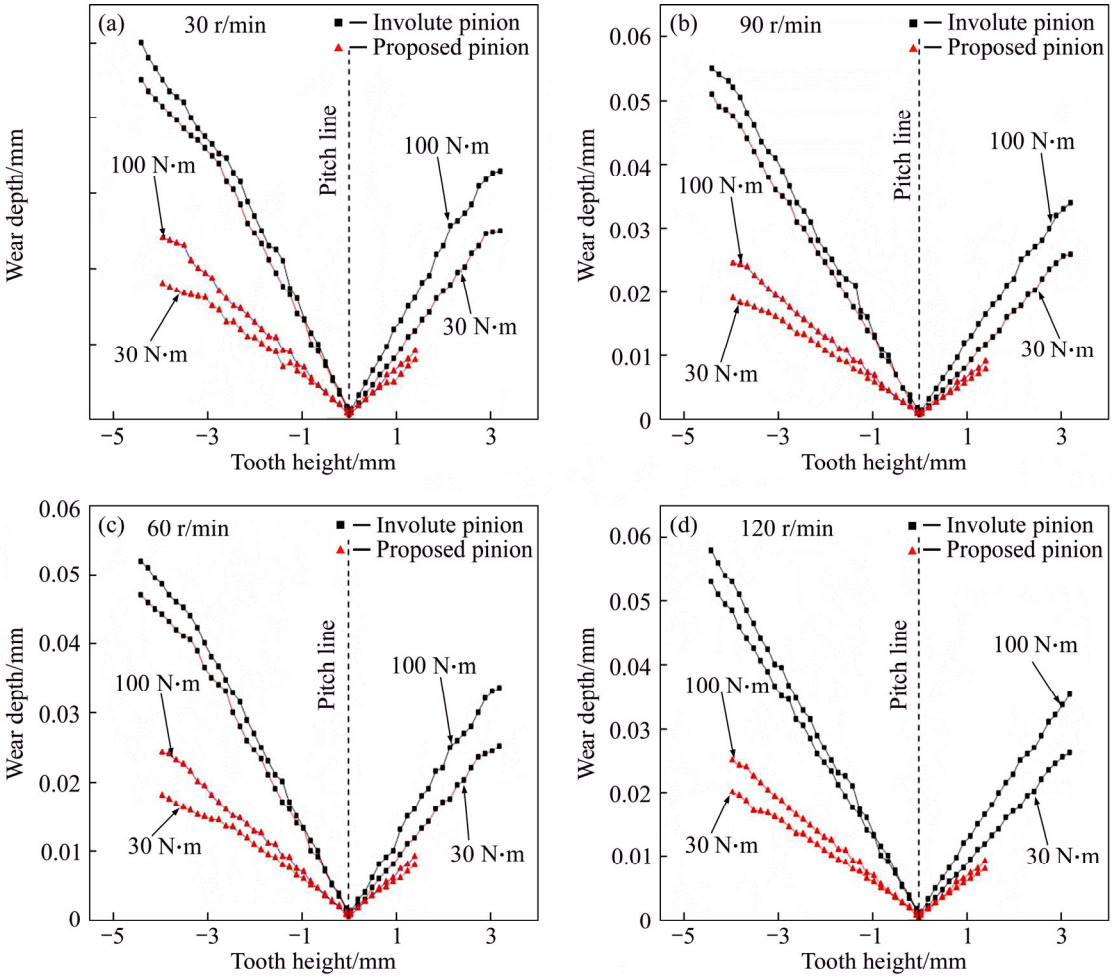

Figure 14 Variation of wear depth of two gears under different output torsional moments and motor speeds: (a) 30 r/mm; (b) 90 r/mm; (c) 60 r/mm; (d) 120 r/mm

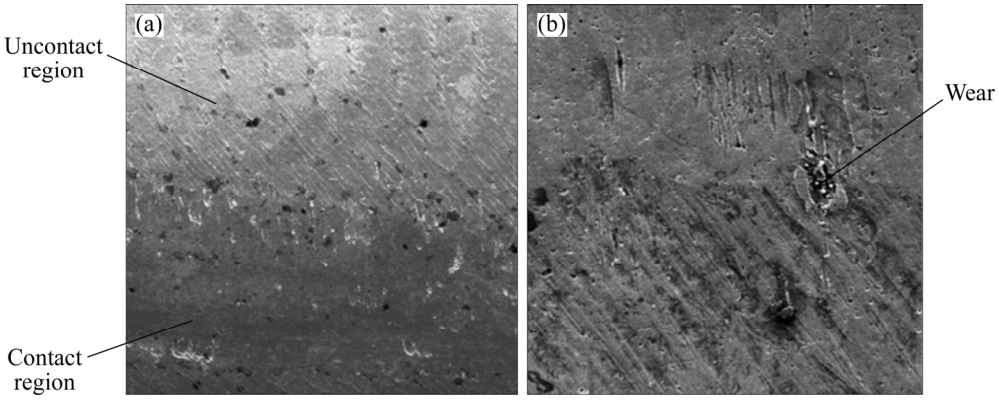

Figure 15 Surface topography of proposed pinion (a) and involute pinion (b)

2) Compared with wear of the involute gear pair with the same design parameters under the same conditions, the proposed gear pair shows better performance.

6 Conclusions

In this work, an internal gear pair with small sliding ratio is proposed which consists of an involute internal gear and a pinion with quadratic curve teeth. The equation of the proposed pinion is presented. Particularly, the contact pattern is point contact and the pinion is generated based on an involute gear. According to the analysis, some conclusions can be drawn:

1) The sliding ratio of the new gear pair is discussed compared with the involute gear pair. The sliding ratio of the new gear is close to zero and much smaller than that of the involute gear, which can reduce wear and improve the transmission performance.

2) The exactitude solid model of the gear pair is established by using MATLAB and solid modeling software UG. According to the exactitude solid model, the motion simulation is performed and validates the correctness of the contact pattern. The separability of center distance of the internal gear pair is presented and a further evaluation of contact stress is made.

3) The internal gear pair was manufactured and inspected for experimental purpose. The efficiency experiment and the contrast experiment with the involute gear pair were performed. The efficiency of the new internal gear is stable at a range about 97.1% to 98.6%.

4) Wear depths of two pinions were measured by measuring center. The results reveal that wear depth is less than 50% of the involute gear pair at any conditions of output torsional moment and motor speed. The internal gear pair is expected to have excellent transmission performance.

5) Two pinions were analyzed by scanning electron microscope after the experiment and the result shows that the tooth surface of the proposed gear becomes smoother at the contact region than that before the experiment. The proposed gear pair shows better performance in wear-resistance than that of the involute gear pair with the same design parameter under the same conditions.

Nomenclature

r Radius of base circle
θ Involute parameter
p Helix parameter
α Rotation angle around the axis
B Tooth width
t Parameter of tooth profile
$\boldsymbol{n}_2$ Normal vector of given surface Σ_1 at contact point
i_{12} Transmission ratio
dx_{Ii}, dy_{Ii}, dz_{Ii}(i=1, 2) coordinate values of the tooth profiles of the gears.

References

[1] PEETERS J L M, DIRK V, PAUL S. Analysis of internal drive train dynamics in a wind turbine [J]. Wind Energy, 2006, 9(1, 2): 141–161.

[2] PATIL S S, KARUPPANAN S, ATANASOVSKA I, WAHAB A A. Contact stress analysis of helical gear pairs, including frictional coefficients [J]. International Journal of Mechanical Sciences, 2014, 85(8): 205–211.

[3] SHENG Zhao-hua, TANG Jin-yuan, CHEN Si-yu, HU Ze-hua. Modal analysis of double-helical planetary gears with numerical and analytical approach [J]. Journal of

Dynamic Systems Measurement & Control, 2015, 137(4): 041012.
[4] ZHANG Yu, YAN Hong-zhi, ZENG Tao, ZENG Yi-yu. Tooth surface geometry optimization of spiral bevel and hypoid gears generated by duplex helical method with circular profile blade [J]. Journal of Central South University, 2016, 23(3): 544–554.
[5] XIA Ji-qiang, SHI Kan, WANG Chun-jie. High-order involute modified noncircular bevel gears [J]. Journal of Advanced Mechanical Design Systems & Manufacturing, 2014, 8(3): 1–15.
[6] SHAO Ren-ping, JIA Pu-rong, DONG Fei-fei. Dynamic characteristics of cracked gear and three-dimensional crack propagation analysis [J]. Proceedings of the Institution of Mechanical Engineers Part C, Journal of Mechanical Engineering Science, 2013, 227(6): 1341–1361.
[7] ZHANG Yuan-shen, HU Xiao-han, LIU Yu-bo, LIU Xiao-hua, CHEN Lei. The study of straight conjugate internal meshing gear pump [J]. Machinery Design & Manufacture, 2010 (6): 138–139. (in Chinese)
[8] XU Wen-bo. Study on the internal meshing and transmission of double-circular-arc gear [D]. Zhengzhou: Zhengzhou Research Institute of Mechanical Engineering, 2012. (in Chinese)
[9] KAHRAMAN A, VIJAYAKAR S. Effect of internal gear flexibility on the quasi-static behavior of a planetary gear set [J]. Journal of Mechanical Design, 2001, 123(3): 408–415.
[10] TUNALIOGLU M Ş, TUC B. Theoretical and experimental investigation of wear in internal gears [J]. Wear, 2014, 309(1, 2): 208–215.
[11] LI Ting, PAN Cun-yun, GAO Fu-dong, Wang Xiao-cong. Research on sliding ratios of conjugate surfaces of two degrees of freedom meshing transmission of spherical gear pair [J]. Journal of Mechanical Design, 2012, 134(9): 255–274.
[12] WANG Jian, LUO Shan-ming, WU Yue. A method for the preliminary geometric design of gear tooth profiles with small sliding coefficients [J]. Journal of Mechanical Design, 2010, 132(5): 1–8.
[13] CHEN Ning-xin. Curvatures and sliding ratios of conjugate surfaces [J]. Journal of Mechanical Design, 1998, 120(1): 126–132.
[14] LIANG Dong, CHEN Bing-kui, GAO Yan-e. Calculation method of sliding ratios for conjugate-curve gear pair and its application [J]. Journal of Central South University, 2015, 22(3): 946–955.
[15] ZHAO Ya-ping, WEI Wen-jun, DONG Xue-zhu, TANG Qiu-hua. Calculation method of sliding ratio for spot contact tooth surfaces and application to crossed helical involute gears [J]. China Mechanical Engineering, 2006, 17(S2): 40–43. (in Chinese)
[16] WANG Zheng. Sliding rate analysis of involute gear teeth [J]. Virology, 1988, 164: 309–17. (in Chinese)
[17] ZHANG Yi-cheng. Study on relative sliding ratio of involute internal gear pair [J]. Journal of Mechanical Transmission, 2001, 25(2): 25–27. (in Chinese)
[18] LIANG Dong, CHEN Bing-kui, GAO Yan-e. The generation principle and mathematical model of a new involute-helix gear drive [J]. Proceedings of Institution of Mechanical Engineers Part C, Journal of Mechanical Engineering Science, 2013, 227(12): 2834–2843.
[19] RADZEVICH S P. Theory of gearing: Kinetics [i.e. kinematics], geometry, and synthesis [M]. United States: CRC Press/Taylor & Francis, 2013.
[20] MICHAELIS K. Gear contact friction [M]. Germany: Springer Berlin Heidelberg, 2014.
[21] DENG Song, HUA Lin, Han Xing-hui, HUANG Song. Finite element analysis of contact fatigue and bending fatigue of a theoretical assembling straight bevel gear pair [J]. Journal of Central South University, 2013, 20(2): 279–292.
[22] AOYAMA T. A study on error compensation on high precision machine tool system using a 2D laser holographic scale system [J]. Journal of Advanced Mechanical Design Systems & Manufacturing, 2012, 6(6): 999–1014.
[23] TANG Jin-yuan, CUI Wei, ZHOU Heng, YIN Feng. Integrity of grinding face-gear with worm wheel [J]. Journal of Central South University, 2016, 23(1): 77–85.
[24] LIN Chao, CAO Xi-jun, FAN Yu, ZENG Dong. Pitch deviation measurement and analysis of curve-face gear pair [J]. Measurement, 2015, 81: 95–101.

(Edited by HE Yun-bin)

中文导读

一种基于小滑动率内齿轮副的理论及实验研究

摘要：基于齿轮滑动率，提出一种点啮合内齿轮副，该齿轮副由渐开线内齿轮和齿廓为二次曲线的外齿轮构成，其中，小齿轮为在渐开线齿轮基础上所构建。提出了齿轮成形方法与数学模型。计算该齿轮副滑动率，并与渐开线齿轮进行对比。讨论齿轮副中心距可分性和接触应力。根据设计参数对齿轮副进行加工和检测。为验证模型的正确性，进行效率试验和与渐开线齿轮副的对比实验。此外，通过扫描电子显微镜分析两种类型小齿轮的表面形貌，并用测量中心测量齿轮磨损深度。实验结果表明，所提出的齿轮副效率稳定在 97.1%到 98.6%之间，磨损程度小于同参数渐开线齿轮的 50%。

关键词：内齿轮；滑动率；二次曲线；磨损